JOURNAL OF FORENSIC SCIENCES

J Forensic Sci, March 2011, Vol. 56, No. 2
doi: 10.1111/j.1556-4029.2010.01680.x
Available online at: onlinelibrary.wiley.com

TECHNICAL NOTE

CRIMINALISTICS

John W. Bond,[1,2] *D.Phil.; Louis N. Eliopulos,*[3] *B.A.; and Thomas F. Brady,*[4] *M.F.S.*

Visualization of Latent Fingermark Corrosion of Brass, Climatic Influence in a Comparison Between the U.K. and Iraq

ABSTRACT: Through a comparison of fingermark sweat corrosion of α phase brass in both the U.K. and Iraq, we show how samples from Iraq have improved fingermark corrosion over U.K. samples that require no additional enhancement prior to visualization. Over 50% of Iraqi samples produced fingermark corrosion with full ridge detail compared with 0% from the U.K. X-ray photoelectron spectroscopy analysis of the fingermark corrosion products showed that Iraqi samples exhibit more dezincification with the Zn:Cu ratio averaging 1:1.82 compared with 1:3.07 for U.K. samples. Auger spectroscopy showed the presence of both zinc oxide and copper (I) oxide. No copper (II) was observed on the surface of the corroded brass. Opportunities to exploit the optical properties of these thin film oxides to enhance the visualization of fingermark corrosion are considered, and the potential to use fingermark corrosion of metal as a means of visualizing fingerprints in war zones is discussed.

KEYWORDS: forensic science, latent fingermark, print visualization, metal surface, electrochemical mechanism, latent fingermark components, climate, detection

When latent fingermarks are deposited on metal surfaces, recent research has focused on fingermark imaging techniques that exploit the chemical reaction that can occur between the metal surface and the fingermark deposit. This reaction, effectively a corrosion of the metal surface, results in a change to both the chemical and physical characteristics of the metal surface (1–4). We have shown how leaving fingermark sweat deposits on planar brass disks in air at room temperature for several days produced sufficient corrosion of the metal to enable the fingermark to be imaged even after the residue of the fingermark deposit had been removed (3).

In addition to visualizing fingermark corrosion on spent brass shell casings (5,6), the corrosive reaction between metal and fingermark sweat might also lend itself to visualizing fingermark corrosion on other weapons, such as improvised explosive devices (IEDs), where a dense, ductile metal, such as copper, gives significant penetration (7).

In this technical note, we compare the extent of corrosion caused by fingermark sweat deposited on brass disks in Iraq with results obtained for sweat deposited in the U.K. We examine first how the differing climates affect the visualization of the corrosion and the ability to enhance this visualization (3). X-ray photoelectron spectroscopy (XPS) and Auger spectroscopy analyses are then carried out to determine the fingermark sweat corrosion products, their relative abundance, and how they vary between U.K. and Iraqi samples. Although pure brass has not been a material of choice for IEDs, brass was selected for this comparison as we have shown previously that it can provide a wide range of visible corrosion between different donors (3).

[1]Scientific Support Unit, Northamptonshire Police, Wootton Hall, Northampton NN4 0JQ, U.K.
[2]Forensic Research Centre, University of Leicester, Leicester LE1 7EA, U.K.
[3]Forensic Consultant Division, U.S. Naval Criminal Investigative Service, NCIS Headquarters, Washington, DC 20388-5380.
[4]Regional Forensic Consultant, U.S. Naval Criminal Investigative Service, PO Box 58, Jacksonville, FL 32212.

Received 19 Nov. 2009; and in revised form 3 Feb. 2010; accepted 2 Mar. 2010.

Experimental Details

Materials and Method

For these experiments, 40 donors in the U.K. and 40 donors in Iraq each provided one finger mark sweat deposit onto 1-mm-thick, 25-mm-diameter α phase brass disks (68 Cu-32 Zn by percentage weight). Prior to fingermark deposition, no cleaning regime was undertaken as the disks were covered with a protective polymer film that was removed immediately prior to fingermark deposition. No artificial stimulation of sweat was employed, such as placing the hand in a plastic bag (8) or wearing a latex glove prior to deposition (9). All samples were left in direct sunlight at room temperature (U.K. = 18 ± 5°C, Iraq = 32 ± 7°C) and relative humidity (U.K. = 68 ± 10%, Iraq = 17 ± 6%) for a period of 12 days; this time period being in keeping with our previous work (3). In this time period, 97 h of sunshine were recorded in Iraq compared with 37 h in the U.K. After the 12-day period, samples were washed in a 0.5 L solution of warm water containing a few drops of commercial detergent and rubbed vigorously with a nonabrasive cloth. This washing regime has been shown to remove effectively the fingermark deposit (but not the corrosion) from the surface of the brass disk (10).

XPS was performed using a VG ESCALab 200d spectrometer (VG Scienta, Hastings, U.K.), Al K α radiation (1486.6 eV), and a

hemispherical analyzer. Individual high-resolution spectra were taken at a pass energy of 50 eV and an energy step of 0.05 eV.

Results and Discussion

The fingermark corrosion arising from each deposit was graded based on the quality of ridge detail that was visualized under natural daylight without any additional enhancement. For this, the grading system used previously (3,4) and devised by Bandey (11) was used and this is reproduced in Table 1.

Figure 1 shows a plot of this grading for both U.K. and Iraqi samples.

It can be seen clearly from Fig. 1 that over 50% of the samples from Iraq gave a grade 4 (full ridge development) compared with 0% from the U.K. This difference was made up from all of the other four groups where, in each group, the number of U.K. samples was greater than the number of samples from Iraq with group 1 having no samples from Iraq compared with 18 from the U.K. A chi-square test showed the difference between U.K. and Iraqi samples for groups 1 and 4 to be statistically significant ($p < 0.001$; [12]).

Figure 2 shows a comparison between the best U.K. (grade 3) and Iraq (grade 4) ridge development with no additional enhancement.

Of the 14 Iraqi samples that failed to give grade 4 ridge development, an attempt was made to enhance the visualization of the corrosion using a technique described previously in which a large electric potential (>1 kV) is applied to the brass sample disk followed by the introduction of a fine conducting powder, which adheres preferentially to areas of corrosion on the sample (3,5,6). As has been reported previously (3), this technique was able to produce additional ridge visualization for samples that had been graded 1 or 2; Fig. 3 showing the change from grade 2 to grade 3 for a sample from Iraq.

It was noted that the majority of samples from Iraq (and all of those that were graded 3 or 4) displayed visible evidence of surface oxidation over the entire surface of the disk. Such oxidation has been observed previously for brass disks that have been subjected to elevated temperatures >*c*. 100°C (3). None of the U.K. disks displayed similar surface oxidation. It is likely that the increased temperature in Iraq resulted in this oxidation as the favorable specific heat capacity of brass (13) would enable the brass to achieve a temperature well above the measured air temperature. The effect that elevated temperature has on the formation of fingermark corrosion products was investigated by conducting XPS and Auger analyses on six sample disks from the highest grouping for both the U.K. and Iraq (three samples from group 4 for Iraq and three samples from group 3 for the U.K.). XPS provides a quantitative measure of the elemental composition, oxidation state, and empirical formula of elements present in the surface layer (<10 nm) of a thin film. In addition, Auger transitions within the XPS spectra can give further information about the surface layer composition (14). While XPS is used routinely in the analysis of surface oxidation of both brass and copper (15,16), it has only been used recently to study the surface effects of fingermark corrosion (17). Each of the six sample disks subject to XPS was analyzed on an area where the fingermark sweat deposit had corroded the brass.

TABLE 1—*Grading system for determining the quality of ridge detail for enhanced fingerprints devised by Bandey (11).*

Grade	Comments
0	No development.
1	No continuous ridges. All discontinuous or dotty.
2	One-third of mark continuous ridges. (Rest no development, dotty.)
3	Two-thirds of mark continuous ridges. (Rest no development, dotty.)
4	Full development. Whole mark continuous ridges.

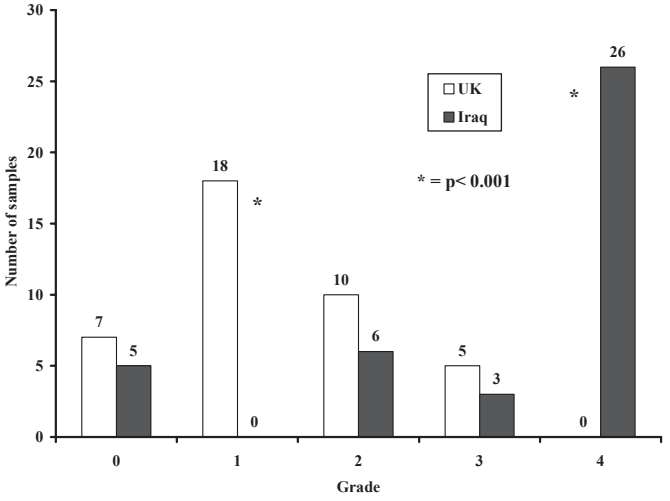

FIG. 1—*Comparison of grading for fingerprint corrosion from 40 fingerprints deposited on brass disks in both the U.K. and Iraq.*

Figure 4 shows typical XPS detail spectra of the copper electron configuration $2p_{3/2}$ and $2p_{1/2}$ sublevels for both a U.K. and an Iraqi disk that gave the highest grading (grade 3 for the U.K. and grade 4 for Iraq).

In Fig. 4, the clear peak at a binding energy of *c*. 933 eV corresponds to the $Cu2p_{3/2}$ sublevel and the peak at *c*. 953 eV corresponds to the $Cu2p_{1/2}$ sublevel. These binding energies are characteristic of both metallic copper and copper (I) oxide (18). The $Cu2p_{3/2}$ peak was deconvoluted using standard Gaussian/Lorentzian functions (19) to reveal whether copper (II) oxide was present as this has a $Cu2p_{3/2}$ peak at *c*. 934 eV, that is, very close to the 933 eV peak. No evidence of copper (II) was found through this deconvolution and this is reinforced in Fig. 4 by the absence of a "shake up" satellite peak at a binding energy *c*. 9 eV higher than the $Cu2p_{3/2}$ peak (20). This "shake up" satellite peak for copper (II) arises because of its incomplete 3d electron orbital enabling a $2p \rightarrow 3d$ charge transfer "shake up" transition. The complete 3d orbital in copper (I) oxide prevents this charge transfer into the d shell and, hence, there is no "shake up" satellite peak for copper (I) oxide (21). Such "shake up" satellite peaks are common in first row d block transition metal compounds (14). Copper metal and copper (I) cannot be resolved by this deconvolution as their binding energy separation is too small (*c*. 0.1 eV). However, they can be distinguished by their auger [Cu ($L_3M_{4,5}M_{4,5}$)] transitions of 568 and 570 eV, respectively, where L_3 represents the core level electron ejected by the incident X-rays and $M_{4,5}$ represents the initial level of both the relaxing electron and the emitted (auger) electron (21). All six samples gave an auger peak confirming the presence of copper (I) oxide.

Metallic zinc and Zn (II) oxide are resolved by the position of their [Zn ($L_3M_{4,5}M_{4,5}$)] auger transitions of 494.7 and 497.8 eV, respectively (15). All six samples gave an auger peak confirming the presence of Zn (II) oxide. Based on atomic percentage, the Zn:Cu ratio was calculated at an average of 1:3.07 for the three U.K. samples and 1:1.82 for the three Iraqi samples.

Thus, the Iraqi samples analyzed by XPS all showed the presence of more zinc (in the form of zinc oxide) on the surface of the corroded brass than the U.K. samples. Such variation in the Zn:Cu

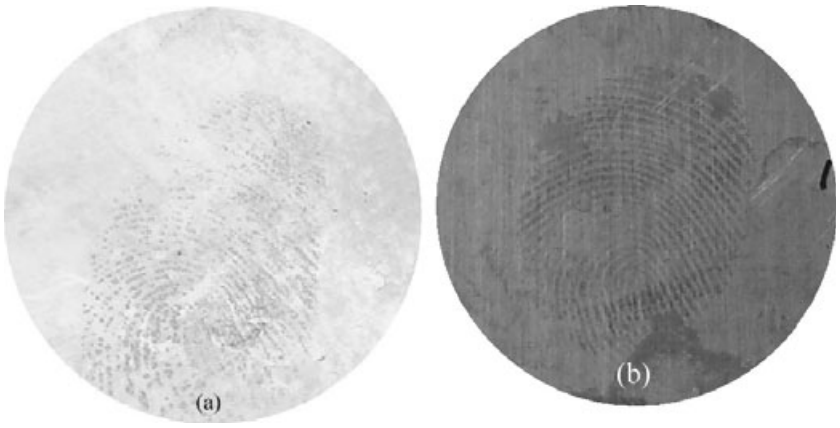

FIG. 2—*Fingerprint corrosion ridge detail for typical samples graded: (a) three from the U.K. and (b) four from Iraq.*

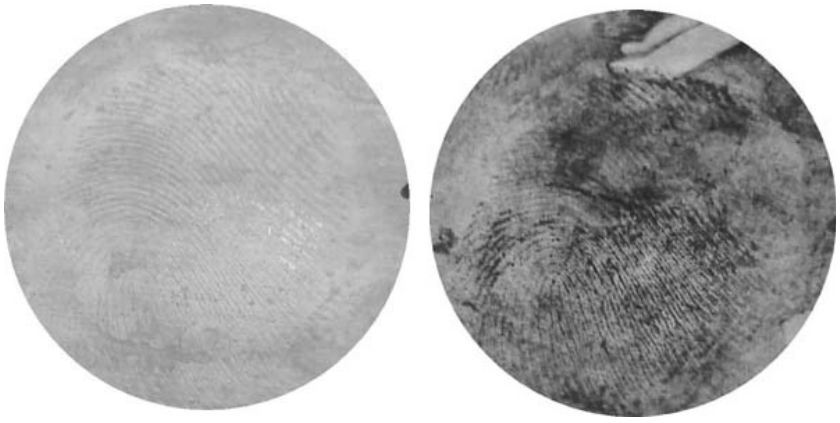

FIG. 3—*Improved fingerprint corrosion visualization for a grade 2 sample from Iraq following the application of an electric potential (−400 V) and conducting powder to the sample.*

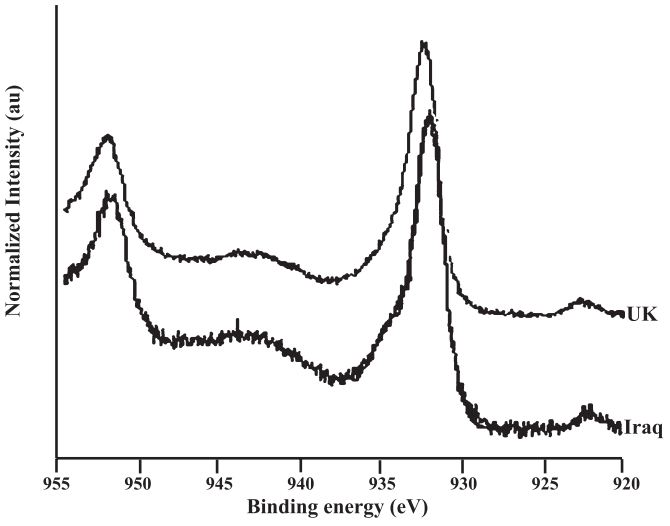

FIG. 4—*Typical X-ray photoelectron spectroscopy detail spectra of the $Cu2p_{3/2}$ and $Cu2p_{1/2}$ peaks for both a U.K. (grade 3) and Iraqi (grade 4) disk.*

ratio on fingermark sweat corroded brass has been observed previously with U.K. samples from different donors (17). Surface concentrations of zinc greater than those expected for uncorroded brass (Zn:Cu = 1:2.2) are indicative of dezincification of the brass (22). This dezincification would increase during electrochemical corrosion of brass at elevated temperatures (22). The ease with which fingermark corrosion could be visualized on Iraqi samples without enhancement (compared with U.K. samples) is clearly an optical effect that is likely to be a combination of the extended light source (natural daylight) and the presence of the zinc oxide thin film on the surface of the corroded brass. As the viewing angle was found to affect significantly the ease of visualization, it is not unreasonable that the thin film of zinc oxide corrosion is producing optical interference. Indeed, the variation in color observed on the surface of the sample disks is most likely due to optical interference from the extended light source. Taking the refractive index of a thin film of zinc oxide to be 2 (23) and a range of viewing angles between 10° and 80°, the film thickness (t) for peak perceptive efficiency of the human eye (550 nm; [24]) equates to 70 nm $\leq t \leq$ 80 nm. This range of t is consistent with values reported for zinc oxide formed during the electrochemical corrosion of α phase brass in an aqueous saline solution (15).

Exploiting the optical properties of the corrosion products may enable enhanced visualization of fingermark ridge detail as thin films of zinc oxide are strongly absorbing at wavelengths $< c$. 400 nm (23,25). In addition, copper (I) oxide is strongly absorbing at wavelengths below 600 nm (26). Recently, Izaki et al. have shown that copper (I) oxide/zinc oxide junctions are absorbing at wavelengths below c. 500 nm (27).

As well as optical absorption, both copper (I) oxide and zinc oxide are luminescent and offer the possibility of fingermark ridge detail visualization through photoluminescence. Beucher et al. used this technique to characterize the oxidation state of copper on oxidized α phase brass (28) and produced a luminescence model for both copper (I) oxide and zinc oxide. Beucher et al. (28) also employed Fourier transform infrared spectroscopy to detect vibrational modes in both oxides, and both of these techniques offer possibilities to enhance the visualization of fingermark corrosion of brass.

Conclusion

Through a comparison of fingermark sweat corrosion of α phase brass in both the U.K. and Iraq, we have shown how samples from Iraq produce an increase in the degree of visible fingermark corrosion that requires no additional enhancement. This increase is because of enhanced dezincification of the brass as a result of the electrochemical reaction between the brass and fingermark sweat taking place at elevated temperatures.

These results invite further work not only to exploit the optical properties of the corrosion products to improve visualization of the fingermark corrosion but also to expand the study to examine disk samples from the various climatic regions/seasonal changes in both Iraq and Afghanistan. Additionally, the placement of fingermarks by test subjects on actual pieces of IED material from Afghanistan would be valuable to assist with the identification of persons in the various regions where IEDs are employed.

Acknowledgments

The authors acknowledge the assistance given by Michael Lake, Supervisory Special Agent, Contingency Response Field Office (Iraq), U.S. Naval Criminal Investigative Service, Brunswick, GA, in conducting this research.

References

1. Williams G, McMurray HN, Worsley DA. Latent fingerprint detection using a scanning Kelvin microprobe. J Forensic Sci 2001;46:1085–92.
2. Williams G, McMurray N. Latent fingermark visualization using a scanning Kelvin probe. Forensic Sci Int 2007;167:102–9.
3. Bond JW. Visualization of latent fingerprint corrosion of metallic surfaces. J Forensic Sci 2008;53:812–22.
4. Bond JW. The thermodynamics of latent fingerprint corrosion of metal elements and alloys. J Forensic Sci 2008;53:1044–52.
5. Bond JW, Heidel C. Visualization of latent fingerprint corrosion on a discharged brass shell casing. J Forensic Sci 2009;54:892–4.
6. Bond JW. Imaging fingerprint corrosion of fired brass shell casings. Rev Sci Instrum 2009;80:075108.
7. Walters WP, Zukas JA. Fundamentals of shaped charges. Danvers, MA: Wiley, 1989.
8. Migron Y, Mandler D. Development of latent fingerprints on unfired cartridges by palladium deposition: a surface study. J Forensic Sci 1997;42:986–92.
9. Migron Y, Hocherman G, Springer E, Almog J, Mandler D. Visualization of sebaceous fingerprints on fired cartridge cases: a laboratory study. J Forensic Sci 1998;43:543–8.
10. Paterson E, Bond JW, Hillman AR. A comparison of cleaning regimes for the effective removal of fingerprint deposits from brass. J Forensic Sci 2010;55:221–4.
11. Bandey HL. Fingerprint development and imaging newsletter: the powders process, study 1. Sandridge, UK: Police Scientific Development Branch, Home Office, 2004; Report No.:54/04.
12. Field A. Discovering statistics using SPSS, 3rd rev. edn. London, UK: Sage, 2009.
13. Kaye GWC, Laby TH. Tables of physical and chemical constants, 16th edn. Harlow, UK: Longman, 1995.
14. Grant JT, Briggs D, editors. Surface analysis by auger and X-ray photoelectron spectroscopy. Chichester: IM Publications, 2003.
15. Kosec T, Merl DK, Milosev I. Impedance and XPS study of benzotriazole films formed on copper, copper-zinc alloys and zinc in chloride solution. Corrosion Sci 2008;50:1987–97.
16. Pallechi I, Bellingeri E, Bernini C, Pellegrino L, Siri AS, Marre D. Epitaxial copper oxide thin films deposited on cubic oxide substrates. J Phys D Appl Phys 2008;41:125407.
17. Bond JW. Determination of the characteristics of a Schottky barrier formed by latent finger mark corrosion of brass. J Phys D Appl Phys 2009;42:235301.
18. Tobin JP, Hirschwald W, Cunningham J. XPS and XAES studies of transient enhancement of CU-1 at CuO surfaces during vacuum outgassing. Appl Surf Sci 1983;16:411–4.
19. Shirley DA. Valence band structure from high resolution X-ray photoelectron spectroscopy (XPS). Phys Rev B 1972;55:4709–14.
20. Al-Kuhaili MF. Characterization of copper oxide thin films deposited by the thermal evaporation of cuprous oxide (Cu_2O). Vacuum 2008;82:623–9.
21. Ghodselahi T, Vesaghi MA, Shafiekhani A, Baghizadeh A, Lameii M. XPS study of the Cu@Cu_2O core shell nanoparticles. Appl Surf Sci 2008;255:2730–4.
22. Tretheway K, Chamberlain J. Corrosion for science and engineering. Harlow, UK: Addison Wesley Longman, 1998.
23. Gumus C, Ozkendir OM, Kavak H, Ufuktepe Y. Structural and optical properties of zinc oxide thin films prepared by spraying pyrolysis method. J Optoelectron Adv Mater 2006;8:299–303.
24. Nelkon M, Parker P. Advanced level physics. Portsmouth, NH: Heinemann, 1974.
25. Ogawa MF, Natsume Y, Hirayama T, Sakata H. Optical absorption edge of zinc oxide films. J Mater Sci Lett 1990;9:1354–6.
26. Richardson TJ, Slack JL, Rubin MD. Electrochromism in copper oxide thin films. Electrochim Acta 2001;46:2281–4.
27. Izaki M, Shinagawa T, Mizuno K, Ida Y, Inaba M, Tasaka A. Electrochemically constructed p-Cu_2On-ZnO heterojunction diode for photovoltaic device. J Phys D Appl Phys 2007;40:3326–9.
28. Beucher E, Lefez B, Lenglet M. Optical determination of cuprous oxide at zinc oxide-metal interface of an oxidized α brass. Phys Stat Sol (a) 1993;136:139–44.

Additional information and reprint requests:
John W. Bond, D.Phil.
Scientific Support Unit
Northamptonshire Police
Wootton Hall
Northampton NN4 0JQ
U.K.
Email: john.bond@northants.police.uk